STROKE

Sensory deprivation after focal ischemia in mice accelerates brain remapping and improves functional recovery through Arc-dependent synaptic plasticity

Andrew W. Kraft,[1] Adam Q. Bauer,[2] Joseph P. Culver,[2,3,4] Jin-Moo Lee[1,2,3]*

Recovery after stroke, a major cause of adult disability, is often unpredictable and incomplete. Behavioral recovery is associated with functional reorganization (remapping) in perilesional regions, suggesting that promoting this process might be an effective strategy to enhance recovery. However, the molecular mechanisms underlying remapping after brain injury and the consequences of its modulation are poorly understood. Focal sensory loss or deprivation has been shown to induce remapping in the corresponding brain areas through activity-regulated cytoskeleton-associated protein (Arc)–mediated synaptic plasticity. We show that targeted sensory deprivation via whisker trimming in mice after induction of ischemic stroke in the somatosensory cortex representing forepaw accelerates remapping into the whisker barrel cortex and improves sensorimotor recovery. These improvements persisted even after focal sensory deprivation ended (whiskers allowed to regrow). Mice deficient in Arc, a gene critical for activity-dependent synaptic plasticity, failed to remap or recover sensorimotor function. These results indicate that post-stroke remapping occurs through Arc-mediated synaptic plasticity and is required for behavioral recovery. Furthermore, our findings suggest that enhancing perilesional cortical plasticity via focal sensory deprivation improves recovery after ischemic stroke in mice.

INTRODUCTION

Stroke is a major cause of disability worldwide (1), resulting in deficits that can be profoundly debilitating (2–4). Although some functional improvements may occur in the weeks to months after the initial ischemic event, recovery is unpredictable and often incomplete (2–4). Several spontaneous brain plasticity mechanisms driving repair and recovery have been uncovered, and enhancing these pathways has been shown to improve behavioral outcomes in animal models of focal brain ischemia (5–8).

In the case of focal ischemia involving the cortex, there is an acute loss of function associated with the infarcted region. Functional recovery occurs in parallel with the appearance of a new functional representation in the perilesional cortex weeks to months after infarction (9–14). This process, termed remapping, has been observed in both animal models and human patients recovering from stroke (15–17). Remapping has been demonstrated not only after lesions limited to sensory or motor cortex but also after infarction of subcortical structures (18). However, it is unclear whether remapping is a necessary step for behavioral recovery. Moreover, the cellular and molecular mechanisms responsible for remapping are only beginning to be elucidated. Early studies examining recovery after motor cortex lesions in nonhuman primates demonstrated that physical activity of the affected limb was required for remapping to occur (9). Subsequent work in mice with genetically engineered calcium indicators revealed that remapping after sensory cortex infarction involved changes in somatic sensory receptivity at the level of individual neurons (11). Thus, sensory remapping may involve the competition of somatosensory input from affected and adjacent somatic regions (with intact sensation) for receptivity of common neurons in the somatosensory cortex.

Amputation of limbs or digits in primates, or trimming of whiskers or visual deprivation in rodents, results in expanded representation of the intact senses into the deprived cortical regions (19–22). In the absence of injury, competition for cortical sensory representation can also occur in the setting of sensory deprivation—a maneuver well known to induce cortical plasticity (21, 22). Although the effects of deprivation on cortical representation may be most marked during development, sensory deprivation also induces plasticity in the adult brain (21, 23–26).

Activity-regulated cytoskeleton-associated protein (Arc) has been demonstrated to play a critical role in experience-dependent synaptic plasticity through coordinated α-amino-3-hydroxy-5-methyl-4-isoxazolepropionic acid receptor (AMPAR) endocytosis (27, 28). Arc gene deletion in mice attenuates long-term depression and long-term potentiation consolidation in situ and memory consolidation in vivo (29). Furthermore, Arc is required for ocular dominance plasticity in the visual cortex during critical period monocular deprivation (30). On the basis of these findings, we hypothesized that focal sensory deprivation after cortical infarction might enhance plasticity, facilitate remapping, and improve behavioral recovery through Arc-dependent mechanisms.

We tested our hypothesis in a mouse model of focal cortical ischemia in the forepaw somatosensory cortex. Targeted sensory deprivation via whisker trimming accelerated remapping into the whisker barrel cortex (adjacent to the infarcted forepaw somatosensory cortex) and improved sensorimotor recovery in mice through Arc-dependent synaptic plasticity.

[1]Department of Neurology, Washington University School of Medicine, 660 South Euclid Avenue, Campus Box 8111, St. Louis, MO 63110, USA. [2]Department of Radiology, Washington University School of Medicine, St. Louis, MO 63110, USA. [3]Department of Biomedical Engineering, Washington University School of Medicine, St. Louis, MO 63110, USA. [4]Department of Physics, Washington University School of Medicine, St. Louis, MO 63110, USA.
*Corresponding author. Email: leejm@wustl.edu

RESULTS

Remapping is accelerated and redirected to the whisker barrel cortex in whisker-deprived mice

Three-month-old male mice were subjected to unilateral somatosensory forepaw cortex (S1FP) photothrombosis (on the left hemisphere,

corresponding to the right forepaw somatosensory representation) and followed for 8 weeks after ischemia. To determine whether post-infarct remapping can be altered by targeted perilesional sensory deprivation, we trimmed all contralesional (right) mystacial whiskers starting 48 hours after ischemia to sensory-deprive the barrel cortex adjacent to infarcted S1FP (on the left hemisphere). Whiskers were kept under 1 mm for the entire recovery time (for 8 weeks). This study consisted of four experimental groups (Fig. 1A): (i) wild-type mice (WT-Control), (ii) WT mice subjected to sensory deprivation (WT-Depriv), (iii) *Arc*−/− mice (Arc-Control), and (iv) *Arc*−/− mice subjected to sensory deprivation (Arc-Depriv). Forepaw mapping and behavioral testing were performed before and at multiple time points after ische-mia (Fig. 1B). S1FP photothrombotic infarct volume and perilesional astrogliosis, measured as glial fibrillary acidic protein (GFAP) expression, were not different between WT-Control and Arc-Control mice (figs. S1 and S2). Throughout the study period, all mice were housed in enriched environments to expand the dynamic range for behavioral recovery.

Optical intrinsic signal (OIS) imaging under anesthesia showed that cutaneous electrical stimulation of the right forepaw resulted in consistent activation of S1FP cortex on the left hemisphere in all groups before photothrombosis (Fig. 1C and figs. S3 to S7A). Photo-thrombosis targeted to left S1FP resulted in markedly reduced evoked right forepaw responses in the first week after injury in all groups (Fig. 1D and figs. S3 to S5). Photothrombosis did not affect the evoked responses of the left forepaw (figs. S7B and S8A) or the right hindpaw in any of the groups (fig. S8B). Evoked right forepaw responses re-appeared 8 weeks after infarction in the regions anterior to the infarct (near motor cortex) in WT-Control mice, suggesting that remapping occurred and involved motor-cortical areas (Fig. 1, C and D). In whisker-deprived mice (WT-Depriv), reappearance of right S1FP maps occurred earlier (4-week time point), and remapping was observed in regions posterior to the infarct, within the whisker barrel cortex (Fig. 1, C and D, and figs. S3 to S5). At 8 weeks after ischemia, the right forepaw evoked response was still present in the whisker cortex; the left forepaw evoked response remained in the same location throughout this time course (figs. S7B, S9, and S10). Thus, focal sensory deprivation influenced both the timing and location of remapping.

Although substantial evidence suggests that cortical plasticity is dependent on the dynamic changes in synaptic structure and function, it is unclear whether similar mechanisms are required for remapping after cortical injury. To determine whether activity-dependent synaptic plasticity was required for post-infarct remapping and recovery, we subjected *Arc*−/− mice (Arc-Control) and whisker-deprived *Arc*−/− mice (Arc-Depriv) to photothrombosis and followed S1FP remapping. In our experiments, baseline preischemic sensory-evoked responses in Arc-Control mice were similar in location and amplitude to those in WT-Control mice (Fig. 1, C and D, and figs. S3 to S5 and S7). Eight weeks after photothrombosis, right forepaw evoked responses were still reduced in both Arc-Control and Arc-Depriv mice (Fig. 1, C and D, and figs. S3 to S5). Collectively, these data show that Arc is required for infarct-induced cortical remapping and suggest that cortical remodeling after focal ischemia shares essential components with mechanisms involved in activity-dependent synaptic plasticity.

Whisker deprivation improves behavioral recovery after focal ischemia

To determine whether whisker deprivation altered sensorimotor be-havioral recovery, we used the cylinder rearing test—an observational
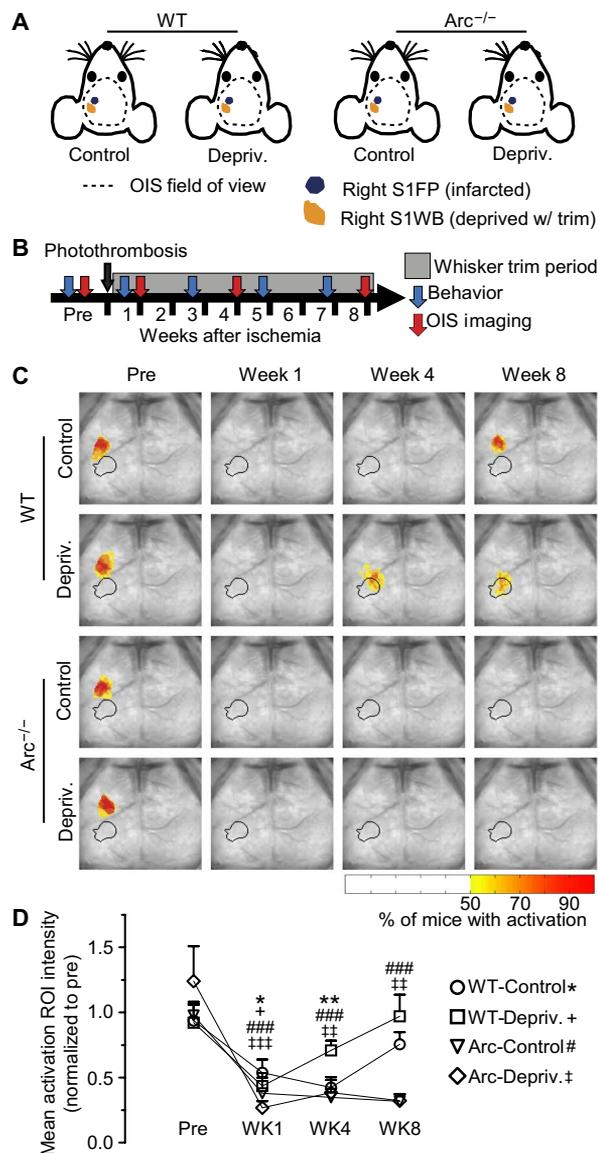

Fig. 1. Whisker deprivation accelerates right forepaw remapping after photo-thrombosis. (**A**) Schematic representation of the experimental groups used in the study: WT, wild-type mice; *Arc*, *Arc* knockout mice; Control, whiskers intact; Depriv, whiskers trimmed. In the OIS field of view (dashed circle), the area subjected to photothrombosis (S1FP, blue) and whisker barrel cortex (S1WB, yellow) is shown. (**B**) Timeline illustrates behavioral testing, OIS imaging, and whisker trimming. (**C**) Activation density heat maps projected onto a white light cortical image shows the area activated by right forepaw stimulation at baseline (Pre) and 1 (WK1), 4 (WK4), and 8 (WK8) weeks after photothrombosis. The whisker barrel cortex, delineated using whisker stimulation–evoked mapping with OIS imaging, is outlined in black. (**D**) Mean activation intensity (calculated for individual mice) after right forepaw stimulation for each group over the recovery time course. Intensity response is determined for each mouse before being group-averaged. *,+$P \le 0.05$, **,‡‡$P \le 0.01$, ###,+++$P \le 0.001$ compared to baseline using repeated-measures analysis of variance (ANOVA). WT-Control, $n = 11$; WT-Depriv, $n = 10$; Arc-Control, $n = 8$; Arc-Depriv, $n = 7$.

sensorimotor test that assesses lateralized forelimb use during sponta-neous exploratory behavior inside a glass cylinder (Fig. 2A). Healthy animals explore the walls of the cylinder while rearing using both forepaws equally. However, immediately after sensory or motor cortex
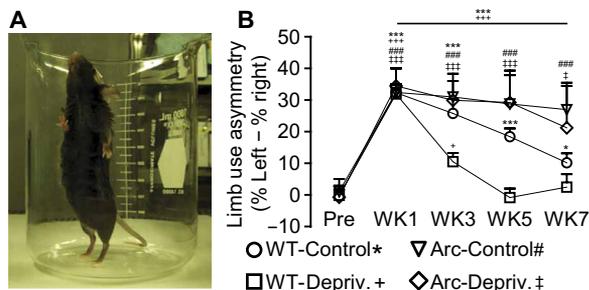
Fig. 2. Whisker deprivation accelerates and enhances behavioral recovery after right S1FP photothrombosis. (**A**) Cylinder rearing test shows forepaw use during exploratory behavior. (**B**) Graph shows limb use asymmetry before (Pre) and 1 (WK1), 3 (WK3), 5 (WK5), and 7 (WK7) weeks after photothrombosis in the experimental groups described in Fig.1A. $*,\ddagger P \leq 0.05$, $***,+++,\#\#\#,\ddagger\ddagger\ddagger P \leq 0.001$ compared to baseline time point (Pre), using repeated-measures ANOVA with Newman-Keuls multiple pairwise comparisons. WT-Control, $n = 22$; WT-Depriv, $n = 16$; Arc-Control, $n = 7$; Arc-Depriv, $n = 7$.

Fig. 3. Regions of remapping demonstrate increased dendritic spine density. (**A**) Cortical dendritic spines (inset, photomicroph of Golgi-Cox–stained spines) were counted at perilesional and distant regions in relation to the area of photothrombosis (blue). Mean spine density is compared between the four groups of mice (WT-Control, WT-Depriv, Arc-Control, and Arc-Depriv) at the distant site (**B**) as well as at anterior (**C**) and posterior (**D**) perilesional sites. Statistical comparisons were performed using ANOVA with Bonferroni correction ($*P \leq 0.05$; $**P \leq 0.01$). WT-Control, $n = 5$; WT-Depriv, $n = 5$; Arc-Control, $n = 4$; Arc-Depriv, $n = 4$.

photothrombosis, mice preferentially use the unaffected limb; this asymmetric forelimb use is followed by recovery of symmetry within 8 weeks after infarction (7, 12, 31). A major advantage of this test is that it does not involve any training—an essential requirement for the examination of $Arc^{-/-}$ mice, which have significant learning deficits (28).

At baseline, all groups demonstrated symmetrical forelimb use (Fig. 2B). S1FP photothrombosis resulted in use asymmetry due to relative decreases in right forelimb use that was consistent across all groups examined (Fig. 2B). In WT-Control mice, limb use symmetry was significantly improved 7 weeks (WK7) after photothrombosis, but the WK7 limb use was still asymmetric compared to baseline, suggesting only partial recovery (Fig. 2B). This time course is in agreement with previous studies using small photothrombotic lesions isolated to the primary sensory cortex (12). In the WT-Depriv mice, recovery showed marked acceleration as symmetry was completely restored 5 weeks after ischemia and persisted to week 7 (Fig. 2B). Thus, focal sensory deprivation via whisker trimming improved both the rate and extent of behavioral recovery. $Arc^{-/-}$ mice (both Arc-Control and Arc-Depriv) showed persistent asymmetry throughout the 7-week timeline, indicating the absence of behavioral recovery (Fig. 2B). Whisker deprivation alone (in the absence of cortical photothrombosis) for 3 weeks did not result in any limb asymmetry (fig. S11).

Dendritic spine density is enhanced in remapped cortex

Turnover of dendritic spines is likely an important mechanism involved in brain repair after focal ischemia. Within hours of an ischemic insult, a marked decrease in perilesional dendritic spine density is observed (32–35), and in the following weeks, spine turnover increases with spine generation outpacing spine removal. This results in spine accumulation and gradual recovery of perilesional spine density (35).

We quantified dendritic spine density 4 weeks after ischemia in layers II/III and IV at three cortical locations (Fig. 3A): (i) distant site (1.5 mm medial to the lesion, in motor cortex, Fig. 3B), (ii) anterior perilesional (near motor cortex, Fig. 3C), and (iii) posterior perilesional (whisker barrel cortex, Fig. 3D). Overall, we found decreased dendritic spine density at the perilesional locations compared to the distant site (fig. S12)—a finding consistent with previous studies (35). However, in the WT-Control mice (no whisker deprivation), spine density in the
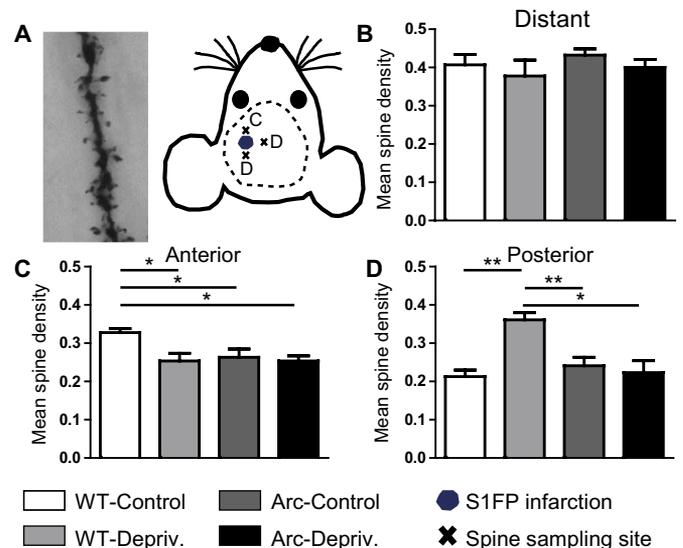
anterior perilesional location (where remapping occurred) was significantly higher than in all other groups (Fig. 3C). In contrast, WT-Depriv mice had increased spine density at the posterior perilesional location (within whisker barrel cortex) compared to all other groups (Fig. 3D). In both WT-Control and WT-Depriv mice, the location of increased spine density corresponded to the region of remapping. The $Arc^{-/-}$ mice (Arc-Control and Arc-Depriv) did not show any increase in spine density at any location examined, regardless of whisker trimming status (Fig. 3, B to D). Collectively, our data demonstrate that cortical regions of remapping are associated with increased dendritic spine density.

Deprivation-induced remapping and behavioral improvement are stable after whisker regrowth

To determine the stability of deprivation-induced remapping and behavioral recovery, we examined remapping and behavioral performance after allowing whisker regrowth. After photothrombosis-induced ischemia, we performed whisker trimming for 8 weeks and then allowed whiskers to regrow for 4 weeks (Fig. 4, A and B), a time previously shown to reverse deprivation-induced cortical-evoked response changes in the uninjured brain (36). Whiskers regrow at a rate of >1 mm per day and were fully grown after 1 week. Forepaw-evoked maps were acquired at 8 (Fig. 4, C and D) and 12 weeks (Fig. 4, E and F) after photothrombosis, and whisker-evoked maps were acquired at 12 weeks (Fig. 4, G and H).

At the 8-week time point, forepaw-evoked responses in WT-Control and WT-Depriv mice were in significantly different locations (Fig. 4I and fig. S13), as seen in the previous experiment (Fig. 1C), which persisted to week 12 (Fig. 4J and fig. S13). Thus, after 4 weeks of whisker regrowth, the location of the forepaw-evoked responses for each group remained in the same location (significant overlap) compared to their

Fig. 4. Whisker deprivation–induced remapping is stable beyond the deprivation period. (**A**) WT mice were subjected to right S1FP (R. S1FP) photothrombosis. Half of the mice underwent right whisker trimming every other day for the first 8 weeks of the experiment; thereafter, trimming was halted and whiskers were allowed to regrow. (**B**) Limb behavior and OIS imaging were performed at the times indicated. (**C** to **H**) Activation density heat maps projected onto a white light cortical image show right S1FP maps, 8 (C and D) and 12 weeks (E and F) after photothrombosis, and right S1WB maps 12 weeks after photothrombosis (G and H) in WT-Control (C, E, and G) and WT-Depriv (D, F, and H) groups. RFP, right forepaw; WB, whisker barrel. (**I** to **O**) Activation heat maps projected onto a white light cortical image showing >65% density response for each map. Map identity is indicated by the label in each image, and dark blue represents overlap between the maps. The >65% threshold was used only for display; statistical comparisons were independent of any threshold. Spatial distribution difference: *$P < 0.0071$ (Bonferroni-corrected); n.s., not significant (see fig. S13 and Materials and Methods for more details). WT-Control, $n = 11$; WT-Depriv, $n = 11$. (**P**) Line graph showing the differences in limb use asymmetry before (Pre) and 1 (WK1), 3 (WK3), 5 (WK5), 7 (WK7), and 11 (WK11) weeks after right S1FP photothrombosis in WT-Control and WT-Depriv mice. *$P \le 0.05$, **$P \le 0.01$, ***, +++$P \le 0.001$; n.s., not significant compared to baseline time point (Pre), using repeated-measures ANOVA with Newman-Keuls multiple pairwise comparisons. WT-Control, $n = 11$; WT-Depriv, $n = 8$.
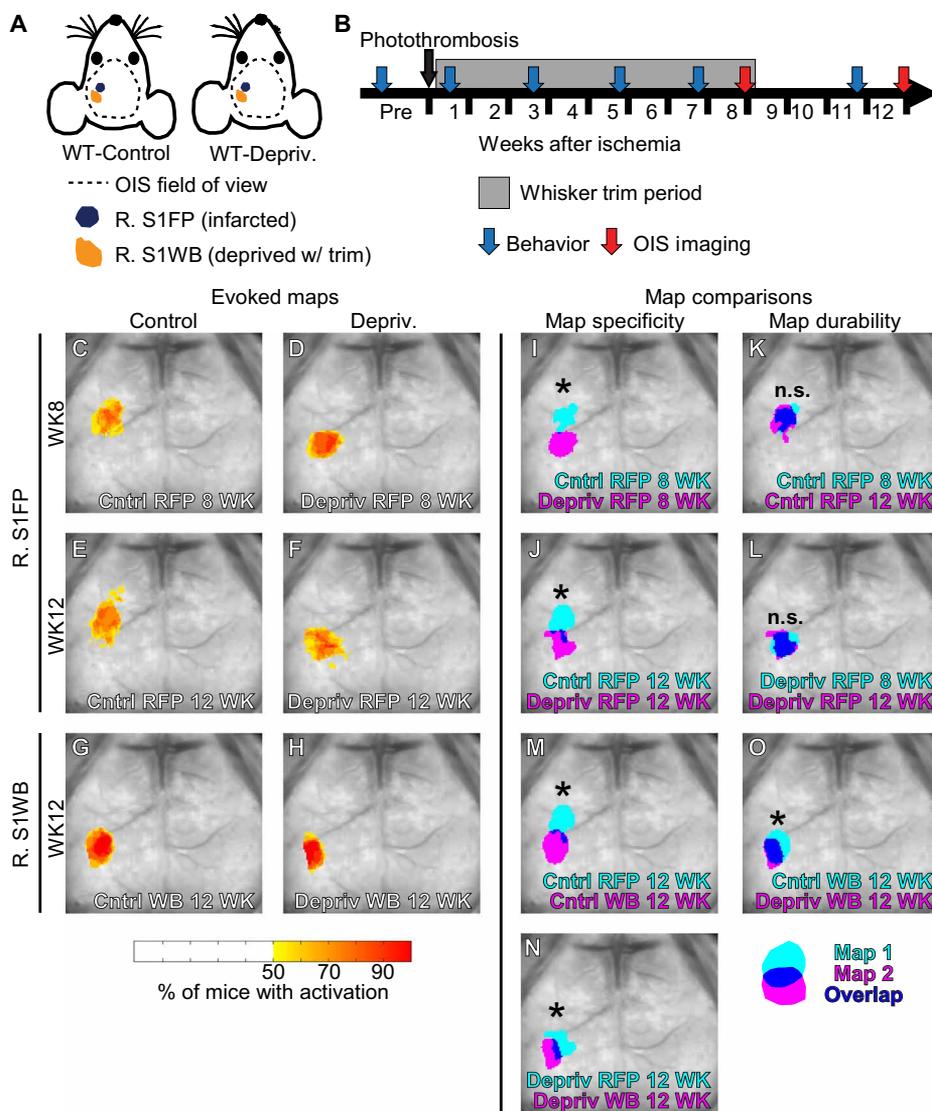
respective 8-week maps (Fig. 4, K and L, and fig. S13). These data suggest that whisker regrowth and concomitant whisker sensory input did not adversely affect the remapped area, which remained stable during this period of regrowth.

To determine the spatial relationship between the remapped region and the whisker sensory area, we superimposed forepaw- and whisker-evoked maps 12 weeks after photothrombosis (Fig. 4, M and N, and fig. S13). Both WT-Control and WT-Depriv groups showed robust responses to whisker stimulation in the S1WB; however, in the WT-Depriv animals, the responsive area was significantly smaller than that of the WT-Control mice (Fig. 4O and fig. S14). The remapped forepaw-evoked response had little overlap with the whisker-evoked responses, and the spatial distributions were statistically distinct (Fig. 4N and fig. S13). Notably, although the display comparisons shown in Fig. 4 (I to O) show the 65% incidence contour, it is important to note that all statistical comparisons were made independent of any % incidence

threshold (see Materials and Methods and fig. S13). Together, these data suggest that whisker deprivation enhances remapping into the whisker somatosensory cortex and that this remapping occurs at the spatial expense of the whisker map. Moreover, we provided evidence

indicating that the remapping remains stable despite whisker regrowth (and sensory input recovery).

To determine whether whisker regrowth altered forepaw use, we performed serial cylinder rearing tests during and after whisker trimming (timeline shown in Fig. 4B). During the period of whisker trimming, the whisker-deprived group showed accelerated and complete recovery by 5 weeks after photothrombosis (Fig. 4P). After whisker regrowth, the improved performance persisted in the whisker-deprived mice (Fig. 4P). These data suggest that adjacent focal sensory deprivation accelerates and improves the extent of behavioral recovery after ischemic injury and that this recovery is durable despite the resumption of sensory input.

DISCUSSION

It has long been speculated that brain plasticity with concomitant functional remapping is important for behavioral recovery after focal brain injury (9, 10, 15–17). Here, we provide evidence that experimental manipulation of cortical plasticity can alter remapping and enhance behavioral recovery. We show that remapping can be directed to specific cortical regions using focal sensory deprivation targeted to perilesional regions. Focal sensory deprivation (via whisker deprivation) resulted in earlier remapping, improved behavioral recovery, and increased synaptic spine density within the remapped areas that persisted after the resumption of sensory input. Furthermore, we show that remapping and behavioral recovery require *Arc*, suggesting that mechanisms involved in experience-related synaptic plasticity play a critical role also in remapping induced by focal injury.

Our finding that sensory deprivation modifies post-ischemic remapping is consistent with the effects of sensory experience in the uninjured brain. More specifically, selective sensory deprivation in both young and mature animals leads to the contraction of deprived sensory cortical representations and concomitant expansion of neighboring, spared cortical representations (20–26, 37, 38). A well-studied example of this phenomenon is ocular dominance plasticity with monocular deprivation, where ocular dominance columns from the normal eye expand into columns representing the deprived eye (22, 26, 37). The same principle applies to the somatosensory system where removal of select whiskers results in expansion of neighboring, spared whisker barrel fields into the deprived barrels (21, 23, 24, 38, 39), and transection of the infraorbital nerve in adult rats results in expansion of the forepaw digit somatosensory representations into the barrel cortex (20). Our data demonstrate that focal sensory deprivation targeted to perilesional cortex can enhance remapping, suggesting that cortical plasticity is heightened by functional loss of the targeted cortical region. Moreover, our data suggest that remapping may occur at the spatial expense of the cortical region targeted for sensory deprivation.

Remapping after photothrombosis has been shown to involve receptivity shifts in individual perilesional neuron responses (11). More specifically, perilesional hindlimb neurons in the primary somatosensory cortex are initially unaffected by somatosensory forepaw cortex photothrombosis and respond only to hindlimb stimulation. However, weeks later, these same perilesional hindlimb cortical neurons are excitable by both forelimb and hindlimb stimulation. Eventually, these neurons become selectively responsive only to forepaw stimulation (11). The dynamic process observed at the single-neuron level reflects what is seen in this remapping study. We speculate that the sensory input from each somatic region influences changes in cortical repre-

sentation. Thus, whisker activity may compete with forepaw activity for cortical representation. Eliminating whisker activity (and thereby a competing stimulus) might allow neurons in the whisker barrel to respond to forepaw stimuli, thereby boosting remapping potential of the forepaw somatosensory cortex.

Although our results show remapping in cortical regions, the precise cellular rewiring that is required for remapping and recovery of function is unclear. It is possible that surviving cortical neurons representing the affected limb form new connections to adjacent cortex, thereby creating a new representation (remapping). Alternatively, it has been suggested that preexisting silent, or subthreshold, thalamocortical synapses may be strengthened to allow remapping to occur (5). Although thalamocortical plasticity has been postulated to be limited in mature mice (40, 41), it is possible that ischemic injury initiates plasticity mechanisms to allow these thalamocortical neurons to extend axons to form new synapses in adjacent surviving cortex. In addition to potentiation of preexisting connections, formation of de novo connections appears to be important as well. In the weeks after cortical infarction, up-regulation of various genes results in robust axonal sprouting that increases cortical connectivity and plays a role in behavioral recovery (6, 8).

Photothrombosis in WT mice without intervention resulted in remapping, suggesting that injury itself may also trigger plasticity and remapping. Studies in animal models show that brain ischemia induces gene and protein expression alterations that are critical for plasticity associated with recovery (6, 8, 42–44). For example, inflammation induced by cerebral ischemia leads to production and elaboration of matrix metalloproteinases that play a critical role in neurovascular remodeling and behavioral recovery weeks after the initial injury (45). Furthermore, ischemia induces perilesional expression of factors that induce axonal sprouting—a critical element of behavioral recovery (6, 8). Our study suggests that endogenous repair mechanisms triggered by the injury can be enhanced to accelerate and improve recovery.

The behavioral recovery advantage of focal perilesional sensory deprivation shown here persisted after the reintroduction of sensory input. The finding that whisker-evoked responses remained robust after deprivation suggests that the whisker somatosensory system is functional. However, it is unclear whether this whisker map contraction reflects compromised whisker sensory function, because this was not formally tested. It should be noted that constraint-induced movement therapy, a standard neurorehabilitative intervention, uses a similar approach (in principle) of movement restriction of the arm contralateral to the paretic arm without causing evident deficits; however, more careful examination is needed to determine the benefit and side effects of deprivation therapies (46–48).

The results in the current study implicate Arc in post-ischemic remapping. Extensive work in experimental models has shown that Arc is involved in cortical plasticity after sensory deprivation in the uninjured brain. For example, Arc has been demonstrated to be required for ocular dominance plasticity with monocular deprivation (30). In addition, in vitro and in vivo studies have demonstrated that Arc affects synaptic plasticity and learning and memory by regulating postsynaptic glutamate receptors (27–29, 49). Excitation at active synapse can induce Arc-mediated AMPAR removal and synaptic weakening at silent or inactive synapses selectively (49); we speculate that this pathway may enable the activity-dependent modulation of select synapses required for the remapping seen after focal cortical ischemia.

Previous work has shown that cortical neuronal activity and sensory-evoked response potentials are not altered in $Arc^{-/-}$ mice (30, 50), suggesting that the experience-dependent plasticity attenuated in $Arc^{-/-}$ mice is not due to generalized neuronal dysfunction but is due to specific disruption of experience-dependent changes. Our data showing that $Arc^{-/-}$ mice have normal baseline somatosensory maps but lack the post-ischemic plasticity that drives remapping and behavioral recovery agree with this hypothesis.

Although we showed that Arc-dependent synaptic plasticity contributes to post-stroke remapping and recovery, our data do not allow us to conclude that Arc plays a role in post-stroke sensory deprivation–enhanced remapping and recovery. Previous studies have shown that genes within the Arc pathway are responsible for sensory deprivation–induced plasticity in the cortical whisker barrels (24, 39). Thus, *Arc*, along with other plasticity-related genes, may be central to remapping regardless of trigger. Moreover, stimuli that enhance remapping may synergistically interact, via Arc or through independent mechanisms, to improve recovery.

Previous examination of perilesional synapses at the level of dendritic spines reveals enhanced spine loss and spine generation (35). This suggests that old connections are replaced with new ones, a process likely critical for receptivity switches in perilesional neurons. Here, we show that post-ischemic spine density recovers selectively in cortical regions where remapping occurs and that *Arc* is required for this increase in dendritic spine density. These results are consistent with previous work from sensory deprivation paradigms (without central nervous system injury) where robust anatomical plasticity was associated with changes in dendritic spines in deprived cortex (51, 52). Similar to what is seen in perilesional cortex after ischemia, sensory deprivation results in increased spine turnover, implicating similar programs for structural and functional connectivity in deprived cortex (51). Arc is known to regulate dendritic spine dynamics through its interaction with actin-regulating proteins in dendritic spines (53–55). Thus, it is not surprising that post-ischemic spine density remains low in *Arc*-deficient mice. However, post-ischemic dendritic spine recovery reflects the new synapses that form through Arc-mediated mechanisms.

Current rehabilitative strategies for motor recovery have focused on increasing use of disabled limbs through "forced use" or constraint-induced movement therapy (46–48). Although this therapeutic strategy takes advantage of use-dependent competition for perilesional cortical representation, it neglects competition from perilesional cortex representing unaffected somatic regions. Thus, rehabilitation might be more effective when coupling forced use with focal deprivation of sensorimotor activity represented in targeted perilesional cortex. Such an approach might involve focal sensory deprivation or motor restraint, whether through mechanical or pharmacological means. Our results suggest that this therapy may only need to be applied temporarily, which is consistent with improvements demonstrated with constraint-induced movement therapy (46–48). However, it is unclear, based on our results, whether deprivation strategies to enhance cortical plasticity are generalizable across other neurological domains (motor or cognitive). Furthermore, whether sensory function in the deprived cortical region is compromised after post-stroke remapping remains uncertain. Current constraint-induced movement therapy approaches have not demonstrated any overt negative impact on functionality after deprivation ended (46–48), but function of the constrained limb has not been carefully examined in clinical trials.

MATERIALS AND METHODS
Study design
The aim of this study was to determine whether post-stroke remapping could be manipulated (both spatially and temporally) to alter behavioral recovery and to determine whether remapping was dependent on activity-dependent synaptic plasticity. Toward this end, we performed photothrombosis targeted at the forepaw somatosensory cortex in mice. Half of the mice were randomly selected to receive focal sensory deprivation (via contralesional whisker trimming), a maneuver known to enhance cortical plasticity in the perilesional cortex (19). Remapping after injury was assessed using OIS imaging (11, 12), and sensorimotor behavioral recovery was assessed using the cylinder rearing test (6, 7, 12). Sample size and specific time points were selected on the basis of previous studies examining behavioral recovery after forepaw somatosensory cortex photothrombosis (6, 7, 12). To determine whether activity-dependent synaptic plasticity was required for remapping and recovery, $Arc^{+/+}$ and $Arc^{-/-}$ mice were subjected to photothrombosis and focal sensory deprivation, and assessed for remapping and behavioral recovery (as described above). In a separate set of experiments, dendritic spines were quantified after Golgi-Cox staining, 4 weeks after photothrombosis in three regions of the cortex: (i) anterior to infarction, (ii) posterior to infarction (in whisker barrel cortex), and (iii) and distant to the infarction (ipsilesional). Sample size was selected on the basis of previous studies examining dendritic spine density dynamics after photothrombosis (34, 35). Image processing and data analysis were performed by an examiner blinded to group and/or genotype. All experiments were performed in accordance with animal protocols approved by the Washington University Animal Studies Committee in compliance with Association for Assessment and Accreditation of Laboratory Animal Care guidelines.

Mice
Colonies of $Arc^{+/+}$ (WT) and $Arc^{-/-}$ mice on a pure C57Bl6/J background (RRID:IMSR_JAX:007662) (50) were raised in standard cages with ad libitum access to food and water in a dedicated mouse facility with a 12-hour/12-hour light/dark cycle.

Imaging windows
Under isoflurane (3.0% induction, 1.5% maintenance), the scalp and periosteal membranes were retracted from the skull, and Plexiglas imaging windows were fixed to the skull with clear metabond dental cement, as described previously (56), to provide a wide field of view of the dorsal cortex. The windows provided a stable imaging platform for serial imaging throughout the study period. Windows were examined for development of infectious abscesses, and any mice that developed window infections were immediately sacrificed in accordance with our animal protocol (WT-Control, $n = 1$; WT-Depriv, $n = 2$; Arc-Control, $n = 0$; Arc-Depriv, $n = 1$).

Whisker trimming
Mice were lightly anesthetized with isoflurane anesthesia, and all right mystacial whiskers were cut to <1 mm with surgical scissors. Mice that did not receive whisker trimming were subjected to the same anesthetic protocol.

Enriched environments and housing
For all recovery studies, mice were housed in 61 cm × 43 cm × 20 cm cages (Nalgene) with the following environmental enrichment components: Mouse Arch, Mouse Huts, Mouse Igloos, Mouse Tunnels, Fast Trac (bio-serv), and EnviroDri crinkle paper.

Kraft *et al.*, *Sci. Transl. Med.* **10**, eaag1328 (2018) 31 January 2018

6 of 10

Photothrombosis

Under isoflurane anesthesia (see above), mice were placed in a stereotactic frame. A 532-nm green diode-pumped solid-state laser (Shanghai Laser & Optics Century) collimated to a 0.5-mm spot was centered on S1FP (0.5 mm anterior to bregma, 2.2 mm left of bregma) at low power (<0.25 mW). The laser was turned off, and mice were then given 200 µl of Rose Bengal dissolved in saline (10 g/liter) via intraperitoneal injection. After 4 min, the laser was powered to 23 mW (centered on S1FP) and targeted to S1FP for 10 min. This approach led to thrombosis of all blood vessels in the target region.

Cylinder rearing

Cylinder rearing recording and analysis were done as previously described (7, 12, 31). Briefly, mice were placed in a 1000-ml glass beaker and video-recorded for 5 min. Group identity was masked, and a custom MATLAB (MathWorks) interface was used to manually analyze videos to determine the amount of time that the (i) right paw, (ii) left paw, or (iii) both paws made contact with the glass walls; the percent of total forepaw contact time was calculated for each condition. Paw-use asymmetry was calculated as (% left paw contact time − % right paw contact time). Any mice that were not spontaneously active during any of the behavioral time points were excluded from analysis (WT-Control, $n = 0$; WT-Depriv, $n = 5$; $Arc^{-/-}$ Control, $n = 1$; $Arc^{-/-}$ Depriv, $n = 0$).

Imaging animal preparation

As reported previously (57), anesthesia was initiated via intraperitoneal injection with a bolus of ketamine-xylazine (5 µl/g; drug concentration: 86.9 mg/kg ketamine, 13.4 mg/kg xylazine dissolved in saline), and animals were allowed 15 min for anesthetic induction. After induction, the animal was placed on a heating pad maintained at 37°C via feedback from a rectal probe (mTCII, Cell MicroControls), and its head was secured in a stereotactic frame. While under ketamine-xylazine anesthesia, forelimb and hindlimb stimulation electrodes were placed (see below); the cortex was positioned in focus of the camera, and the animals were then transitioned to isoflurane anesthesia (<0.5%) for stimulation studies.

Paw stimulation

Transcutaneous electrical stimulation was applied to the forepaw or hindpaw by placing microvascular clips (Roboz) on either side of the wrists or ankles. Electrical stimulation was provided in a block design (model 2100, A-M Systems) with the following parameters: 5-s rest, 1-s stimulation (0.5 mA, 5-ms duration, 100 Hz), and 24-s rest as previously described in other S1FP remapping studies (11, 12).

Whisker stimulation

Whiskers were stimulated via mechanical displacement by placing all mystacial whiskers through an aluminum screen attached to a piezoelectric bending actuator (Piezo Systems). A 2° anterior direction deflection occurred for 5 ms, and the piezo was allowed to fall back to the neutral position. This was presented at 10 Hz with the following parameters: 5-s rest and 1-s stimulation.

Image acquisition

Sequential illumination was provided at four wavelengths by a ring of light-emitting diodes (LEDs) placed about 10 cm above the mouse's head. The field of view included most of the cerebral cortex (about 1 cm^2). Diffuse reflected light was detected by a cooled, frame-transfer electron-multiplying charge-coupled device camera (iXon 897, Andor Technology); the LED ring and the camera were time-synchronized and controlled via computer using custom-written software (MATLAB, MathWorks) at a full frame rate of 30 Hz.

Image processing

Data from all mice were subjected to an initial quality check before spectroscopic analysis. Data blocks in which reflected light level intensity (mean value over the brain) varied as a function of time by greater than 1% for any wavelength were excluded from further analysis. Further, data blocks that had movement contamination were excluded. For subsequent analysis, image light intensity at each wavelength was interpreted using the modified Beer-Lambert law, usually expressed as follows: $\Phi(\mathbf{r},t) = \Phi_0 * \exp(-\Delta\mu_a(\mathbf{r},t)*L)$. Here, $\Phi(\mathbf{r},t)$ is the measured light intensity, Φ_0 is the baseline light intensity, $\Delta\mu_a(\mathbf{r},t)$ is the change in absorption coefficient due to hemodynamic changes, and L is the optical path length factor for photons in the tissue (58). Values were normalized relative to the average light intensity at each pixel, resulting in differential measures of absorption at each wavelength at each pixel: $\Delta\mu_{a,\lambda}(\mathbf{r},t) = -\ln(\Phi_\lambda(\mathbf{r},t)/<\Phi_{0\lambda}(\mathbf{r},t)>)/L_\lambda$. Absorption coefficient data were converted to hemoglobin (Hb) concentration changes by inverting the system of equations, $\Delta\mu_{a,\lambda}(\mathbf{r},t) = E_{\lambda,i}\Delta[Hb_i](\mathbf{r},t)$ (where E is the extinction coefficient matrix and i runs over Hb species). This inversion was performed using least-squares methods, yielding changes in oxygenated Hb (oxy-Hb) at each pixel at each time point. Each pixel's time series was downsampled from 30 to 1 Hz, and all further analysis was performed only on those pixels labeled as brain using a manually constructed brain mask. The time traces of all pixels defined as brain were averaged to create a global brain signal. This global signal was regressed from every pixel's time trace to remove global sources of variance; global signal regression was applied independently on each stimulation block. Because the spectral content of the OIS signal is known to be roughly "1/f," we excluded runs in which 50% of the power of the regressed data was found above 0.04 Hz to exclude data strongly contaminated by oscillatory vascular artifact (59). Thirty-four percent of all imaging blocks were rejected.

Creating somatosensory maps

Oxy-Hb was used for this study because it offers the greatest contrast to noise of all of our spectral components (fig. S15). For each mouse, stimulation blocks were averaged together. From that average response, baseline images (1 s before stimulation) were subtracted from post-stimulation images (2 s after stimulation) to generate the response image. All pixels that were >50% of the maximum amplitude (for each mouse at each time point) were defined as activated as reported previously (11, 12). To create individual binary activation maps, a minimum intensity threshold of 35% of the respective baseline amplitude (averaged over all groups) was required for pixels to be included [this was required to view activation density (percent incidence) maps at the group level]. Percent maps were calculated at the group level by determining the percentage of mice for which each pixel was activated. Mean intensity maps were generated by averaging the intensity maps together without applying a minimum intensity cutoff. Maps of P values were determined via Student's t test between all baseline and activated oxy-Hb images for all group members at each time point.

Image co-registration

Image sequences of each mouse (as well as the brain mask for each mouse) were affine-transformed to a common atlas space determined by the positions of the junction between the coronal suture and sagittal

Kraft *et al.*, *Sci. Transl. Med.* **10**, eaag1328 (2018) 31 January 2018

7 of 10

suture (posterior to the olfactory bulb and cerebrum along midline) and lambda as we have done previously (*60*). Bregma was not visible in all mice and was calculated on the basis of the above two anatomical landmarks. The anterior-posterior stretch was set equal to the medial-lateral stretch, and all transformed images were centered at bregma. The intersection of every brain mask was calculated and made symmetric by reflection across the midline, allowing all subsequent comparisons to be performed on shared brain areas across all mice.

Dendritic spines

Brains were harvested from all groups 25 days after photothrombosis. The Hito Golgi-Cox OptimStain (Hitobiotec) was used to label spines per kit instructions. Brains were embedded in low–melting point gelatin, sliced coronally at 200 µm with a vibratome, and mounted on gelatin-coated slides. Spines were examined in layers II/III and IV. Images were taken at 67× using MicroBrightField Stereology to systematically collect image stacks (25 images per site, 1-µm separation) and generate minimum intensity projections (MIPs). Three MIPs were collected at each sampled location, resulting in an average of 570 spines being imaged per mouse at each location. All spines in the image areas were analyzed. Spine counting and dendrite length were performed on MIPs in ImageJ. For each mouse, a spine density was calculated at each sample location. At each location, spine density was compared across groups.

Histology

Seven days after S1FP infarction, mice were deeply anesthetized and transcardiac perfusion with phosphate-buffered saline followed by 4% paraformaldehyde (PFA) was performed. Brains were submerged in 4% PFA for 24 hours and then kept in cryoprotectant solution for 72 hours before slicing. Brains were sliced at a thickness of 50 µm on a sliding microtome. To determine infarction volume, slices were stained with cresyl violet. Stained sections were imaged with a NanoZoomer, and infarction volume was quantified in ImageJ. To examine astrogliosis, GFAP immunostaining was performed using anti-GFAP antibodies (Sigma) and developed using the 3,3′-diaminobenzidine ABC developing kit (Vector Laboratories). Perilesional images of GFAP-labeled sections were taken with a 40× objective using MicroBrightField Stereology to systematically collect image stacks and generate MIPs. MIPs were intensity-thresholded, and % area of GFAP immunoreactivity was calculated for each mouse.

Statistical analysis

For evoked maps, P values were calculated for each pixel by comparing Oxy-Hb values at baseline and after stimulus using all images within each group at each time point. Clusters of 75 or more pixels with uncorrected P values of $<1 \times 10^{-10}$ were considered statistically significant. For cylinder rearing testing, differences between groups were analyzed using one-way ANOVA with repeated measures and Newman-Keuls multiple pairwise comparisons as has been done previously (*7*). The level of significance was set at $P < 0.05$. For spine density analysis, differences between groups were analyzed using two-way ANOVA with Bonferroni correction for multiple comparisons, and the level of significance was set at $P < 0.05$. For infarction volume and astrogliosis studies, Student's t test was used and the level of significance was set at $P < 0.05$. Statistical map comparisons (Fig. 4, I to O, and fig. S13) were performed by summing the dot products for the % incidence maps for the two maps being compared (the sum of the element-wise produce of both % incidence maps being compared).

This produced a single value, termed "overlap," that was used as the test statistic. An overlap null distribution for each comparison was calculated by calculating the overlap for 10,000 random groupings of the mice involved in the comparison (fig. S8). Statistical significance was set at $P < 0.007$ ($P < 0.05$ per seven comparisons).

SUPPLEMENTARY MATERIALS

www.sciencetranslationalmedicine.org/cgi/content/full/10/426/eaag1328/DC1
Fig. S1. *Arc* gene deletion does not affect infarct volume.
Fig. S2. *Arc* gene deletion does not alter perilesional reactive astrocytosis.
Fig. S3. Full-range activation heat maps mirror thresholded activation maps.
Fig. S4. Mean oxy-Hb intensity maps are similar to activation heat maps.
Fig. S5. *P* value maps show accelerated remapping into the whisker barrel cortex in sensory-deprived mice.
Fig. S6. Baseline right S1FP activation intensity is similar in all groups.
Fig. S7. Baseline forepaw activation is similar in location for all groups of mice.
Fig. S8. Left S1FP and right hindpaw (S1HP) activations remain intact before and after injury.
Fig. S9. Left S1FP activation remains intact throughout injury and recovery.
Fig. S10. Right S1FP remaps after focal ischemia, but left S1FP remains stable throughout the time course.
Fig. S11. Whisker deprivation does not affect limb use symmetry.
Fig. S12. Dendritic spine density is lower in perilesional cortex compared to distant cortical regions.
Fig. S13. Right S1FP maps remain stable after whisker regrowth.
Fig. S14. Right S1WB area is smaller in WT-Depriv compared to WT-Control groups.
Fig. S15. Oxy-Hb contrast demonstrates the greatest signal-to-noise ratio of all spectral components.

REFERENCES AND NOTES

1. E. J. Benjamin, M. J. Blaha, S. E. Chiuve, M. Cushman, S. R. Das, R. Deo, S. D. de Ferranti, J. Floyd, M. Fornage, C. Gillespie, C. R. Isasi, M. C. Jiménez, L. C. Jordan, S. E. Judd, D. Lackland, J. H. Lichtman, L. Lisabeth, S. Liu, C. T. Longenecker, R. H. Mackey, K. Matsushita, D. Mozaffarian, M. E. Mussolino, K. Nasir, R. W. Neumar, L. Palaniappan, D. K. Pandey, R. R. Thiagarajan, M. J. Reeves, M. Ritchey, C. J. Rodriguez, G. A. Roth, W. D. Rosamond, C. Sasson, A. Towfighi, C. W. Tsao, M. B. Turner, S. S. Virani, J. H. Voeks, J. Z. Willey, J. T. Wilkins, J. H. Wu, H. M. Alger, S. S. Wong, P. Muntner; American Heart Association Statistics Committee and Stroke Statistics Subcommittee, Heart disease and stroke statistics—2017 update: A report from the American Heart Association. *Circulation* **135**, e146–e603 (2017).
2. A. Kertesz, P. McCabe, Recovery patterns and prognosis in aphasia. *Brain* **100** Pt 1, 1–18 (1977).
3. D. B. Hier, J. Mondlock, L. R. Caplan, Recovery of behavioral abnormalities after right hemisphere stroke. *Neurology* **33**, 345–350 (1983).
4. P. W. Duncan, L. B. Goldstein, D. Matchar, G. W. Divine, J. Feussner, Measurement of motor recovery after stroke. Outcome assessment and sample size requirements. *Stroke* **23**, 1084–1089 (1992).
5. T. H. Murphy, D. Corbett, Plasticity during stroke recovery: From synapse to behaviour. *Nat. Rev. Neurosci.* **10**, 861–872 (2009).
6. S. Li, E. H. Nie, Y. Yin, L. I. Benowitz, S. Tung, H. V. Vinters, F. R. Bahjat, M. P. Stenzel-Poore, R. Kawaguchi, G. Coppola, S. T. Carmichael, GDF10 is a signal for axonal sprouting and functional recovery after stroke. *Nat. Neurosci.* **18**, 1737–1745 (2015).
7. A. N. Clarkson, B. S. Huang, S. E. Macisaac, I. Mody, S. T. Carmichael, Reducing excessive GABA-mediated tonic inhibition promotes functional recovery after stroke. *Nature* **468**, 305–309 (2010).
8. S. Li, J. J. Overman, D. Katsman, S. V. Kozlov, C. J. Donnelly, J. L. Twiss, R. J. Giger, G. Coppola, D. H. Geschwind, S. T. Carmichael, An age-related sprouting transcriptome provides molecular control of axonal sprouting after stroke. *Nat. Neurosci.* **13**, 1496–1504 (2010).
9. R. J. Nudo, G. W. Milliken, W. M. Jenkins, M. M. Merzenich, Use-dependent alterations of movement representations in primary motor cortex of adult squirrel monkeys. *J. Neurosci.* **16**, 785–807 (1996).
10. C. Xerri, M. M. Merzenich, B. E. Peterson, W. Jenkins, Plasticity of primary somatosensory cortex paralleling sensorimotor skill recovery from stroke in adult monkeys. *J. Neurophysiol.* **79**, 2119–2148 (1998).
11. I. R. Winship, T. H. Murphy, In vivo calcium imaging reveals functional rewiring of single somatosensory neurons after stroke. *J. Neurosci.* **28**, 6592–6606 (2008).
12. C. E. Brown, K. Aminoltejari, H. Erb, I. R. Winship, T. H. Murphy, In vivo voltage-sensitive dye imaging in adult mice reveals that somatosensory maps lost to stroke are replaced over weeks by new structural and functional circuits with prolonged modes

Kraft *et al.*, *Sci. Transl. Med.* **10**, eaag1328 (2018)   31 January 2018

8 of 10

of activation within both the peri-infarct zone and distant sites. *J. Neurosci.* **29**, 1719–1734 (2009).

13. R. M. Dijkhuizen, J. Ren, J. B. Mandeville, O. Wu, F. M. Ozdag, M. A. Moskowitz, B. R. Rosen, S. P. Finklestein, Functional magnetic resonance imaging of reorganization in rat brain after stroke. *Proc. Natl. Acad. Sci. U.S.A.* **98**, 12766–12771 (2001).

14. J. A. Jablonka, K. Burnat, O. W. Witte, M. Kossut, Remapping of the somatosensory cortex after a photothrombotic stroke: Dynamics of the compensatory reorganization. *Neuroscience* **165**, 90–100 (2010).

15. C. Weiller, F. Chollet, K. J. Friston, R. J. Wise, R. S. Frackowiak, Functional reorganization of the brain in recovery from striatocapsular infarction in man. *Ann. Neurol.* **31**, 463–472 (1992).

16. S. C. Cramer, G. Nelles, R. R. Benson, J. D. Kaplan, R. A. Parker, K. K. Kwong, D. N. Kennedy, S. P. Finklestein, B. R. Rosen, A functional MRI study of subjects recovered from hemiparetic stroke. *Stroke* **28**, 2518–2527 (1997).

17. H. Reddy, N. De Stefano, A. Mortilla, A. Federico, P. M. Matthews, Functional reorganization of motor cortex increases with greater axonal injury from CADASIL. *Stroke* **33**, 502–508 (2002).

18. R. M. Dijkhuizen, A. B. Singhal, J. B. Mandeville, O. Wu, E. F. Halpern, S. P. Finklestein, B. R. Rosen, E. H. Lo, Correlation between brain reorganization, ischemic damage, and neurologic status after transient focal cerebral ischemia in rats: A functional magnetic resonance imaging study. *J. Neurosci.* **23**, 510–517 (2003).

19. M. M. Merzenich, R. J. Nelson, M. P. Stryker, M. S. Cynader, A. Schoppmann, J. M. Zook, Somatosensory cortical map changes following digit amputation in adult monkeys. *J. Comp. Neurol.* **224**, 591–605 (1984).

20. K. Korodi, J. Toldi, Does the cortical representation of body parts follow both injury to the related sensory peripheral nerve and its regeneration? *Neuroreport* **9**, 771–774 (1998).

21. K. Fox, Anatomical pathways and molecular mechanisms for plasticity in the barrel cortex. *Neuroscience* **111**, 799–814 (2002).

22. T. K. Hensch, Critical period plasticity in local cortical circuits. *Nat. Rev. Neurosci.* **6**, 877–888 (2005).

23. S. Glazewski, M. McKenna, M. Jacquin, K. Fox, Experience-dependent depression of vibrissae responses in adolescent rat barrel cortex. *Eur. J. Neurosci.* **10**, 2107–2116 (1998).

24. S. Glazewski, C.-M. Chen, A. Silva, K. Fox, Requirement for α-CaMKII in experience-dependent plasticity of the barrel cortex. *Science* **272**, 421–423 (1996).

25. N. B. Sawtell, M. Y. Frenkel, B. D. Philpot, K. Nakazawa, S. Tonegawa, M. F. Bear, NMDA receptor-dependent ocular dominance plasticity in adult visual cortex. *Neuron* **38**, 977–985 (2003).

26. Y. Tagawa, P. O. Kanold, M. Majdan, C. J. Shatz, Multiple periods of functional ocular dominance plasticity in mouse visual cortex. *Nat. Neurosci.* **8**, 380–388 (2005).

27. E. Korb, S. Finkbeiner, Arc in synaptic plasticity: From gene to behavior. *Trends Neurosci.* **34**, 591–598 (2011).

28. S. Chowdhury, J. D. Shepherd, H. Okuno, G. Lyford, R. S. Petralia, N. Plath, D. Kuhl, R. L. Huganir, P. F. Worley, Arc/Arg3.1 interacts with the endocytic machinery to regulate AMPA receptor trafficking. *Neuron* **52**, 445–459 (2006).

29. N. Plath, O. Ohana, B. Dammermann, M. L. Errington, D. Schmitz, C. Gross, X. Mao, A. Engelsberg, C. Mahlke, H. Welzl, U. Kobalz, A. Stawrakakis, E. Fernandez, R. Waltereit, A. Bick-Sander, E. Therstappen, S. F. Cooke, V. Blanquet, W. Wurst, B. Salmen, M. R. Bösl, H. P. Lipp, S. G. Grant, T. V. Bliss, D. P. Wolfer, D. Kuhl, Arc/Arg3.1 is essential for the consolidation of synaptic plasticity and memories. *Neuron* **52**, 437–444 (2006).

30. C. L. McCurry, J. D. Shepherd, D. Tropea, K. H. Wang, M. F. Bear, M. Sur, Loss of Arc renders the visual cortex impervious to the effects of sensory experience or deprivation. *Nat. Neurosci.* **13**, 450–457 (2010).

31. Y. K. Baskin, W. D. Dietrich, E. J. Green, Two effective behavioral tasks for evaluating sensorimotor dysfunction following traumatic brain injury in mice. *J. Neurosci. Methods* **129**, 87–93 (2003).

32. B. B. Johansson, P. V. Belichenko, Neuronal plasticity and dendritic spines: Effect of environmental enrichment on intact and postischemic rat brain. *J. Cereb. Blood Flow Metab.* **22**, 89–96 (2002).

33. S. Zhang, J. Boyd, K. Delaney, T. H. Murphy, Rapid reversible changes in dendritic spine structure in vivo gated by the degree of ischemia. *J. Neurosci.* **25**, 5333–5338 (2005).

34. C. E. Brown, C. Wong, T. H. Murphy, Rapid morphologic plasticity of peri-infarct dendritic spines after focal ischemic stroke. *Stroke* **39**, 1286–1291 (2008).

35. C. E. Brown, P. Li, J. D. Boyd, K. R. Delaney, T. H. Murphy, Extensive turnover of dendritic spines and vascular remodeling in cortical tissues recovering from stroke. *J. Neurosci.* **27**, 4101–4109 (2007).

36. D. B. Polley, C. H. Chen-Bee, R. D. Frostig, Two directions of plasticity in the sensory-deprived adult cortex. *Neuron* **24**, 623–637 (1999).

37. T. N. Wiesel, D. H. Hubel, Comparison of the effects of unilateral and bilateral eye closure on cortical unit responses in kittens. *J. Neurophysiol.* **28**, 1029–1040 (1965).

38. A. Skibinska, S. Glazewski, K. Fox, M. Kossut, Age-dependent response of the mouse barrel cortex to sensory deprivation: A 2-deoxyglucose study. *Exp. Brain Res.* **132**, 134–138 (2000).

39. S. Glazewski, A. L. Barth, H. Wallace, M. McKenna, A. Silva, K. Fox, Impaired experience-dependent plasticity in barrel cortex of mice lacking the alpha and delta isoforms of CREB. *Cereb. Cortex* **9**, 249–256 (1999).

40. T. A. Woolsey, J. R. Wann, Areal changes in mouse cortical barrels following vibrissal damage at different postnatal ages. *J. Comp. Neurol.* **170**, 53–66 (1976).

41. H. Van der Loos, T. A. Woolsey, Somatosensory cortex: Structural alterations following early injury to sense organs. *Science* **179**, 395–398 (1973).

42. S. T. Carmichael, Cellular and molecular mechanisms of neural repair after stroke: Making waves. *Ann. Neurol.* **59**, 735–742 (2006).

43. S. Li, S. T. Carmichael, Growth-associated gene and protein expression in the region of axonal sprouting in the aged brain after stroke. *Neurobiol. Dis.* **23**, 362–373 (2006).

44. S. T. Carmichael, I. Archibeque, L. Luke, T. Nolan, J. Momiy, S. Li, Growth-associated gene expression after stroke: Evidence for a growth-promoting region in peri-infarct cortex. *Exp. Neurol.* **193**, 291–311 (2005).

45. B.-Q. Zhao, S. Wang, H.-Y. Kim, H. Storrie, B. R. Rosen, D. J. Mooney, X. Wang, E. H. Lo, Role of matrix metalloproteinases in delayed cortical responses after stroke. *Nat. Med.* **12**, 441–445 (2006).

46. E. Taub, J. E. Crago, L. D. Burgio, T. E. Groomes, E. W. Cook III, S. C. DeLuca, N. E. Miller, An operant approach to rehabilitation medicine: Overcoming learned nonuse by shaping. *J. Exp. Anal. Behav.* **61**, 281–293 (1994).

47. W. H. R. Miltner, H. Bauder, M. Sommer, C. Dettmers, E. Taub, Effects of constraint-induced movement therapy on patients with chronic motor deficits after stroke: A replication. *Stroke* **30**, 586–592 (1999).

48. S. L. Wolf, D. E. Lecraw, L. A. Barton, B. B. Jann, Forced use of hemiplegic upper extremities to reverse the effect of learned nonuse among chronic stroke and head-injured patients. *Exp. Neurol.* **104**, 125–132 (1989).

49. H. Okuno, K. Akashi, Y. Ishii, N. Yagishita-Kyo, K. Suzuki, M. Nonaka, T. Kawashima, H. Fujii, S. Takemoto-Kimura, M. Abe, R. Natsume, S. Chowdhury, K. Sakimura, P. F. Worley, H. Bito, Inverse synaptic tagging of inactive synapses via dynamic interaction of Arc/Arg3.1 with CaMKIIβ. *Cell* **149**, 886–898 (2012).

50. K. H. Wang, A. Majewska, J. Schummers, B. Farley, C. Hu, M. Sur, S. Tonegawa, In vivo two-photon imaging reveals a role of arc in enhancing orientation specificity in visual cortex. *Cell* **126**, 389–402 (2006).

51. A. Holtmaat, L. Wilbrecht, G. W. Knott, E. Welker, K. Svoboda, Experience-dependent and cell-type-specific spine growth in the neocortex. *Nature* **441**, 979–983 (2006).

52. A. Majewska, M. Sur, Motility of dendritic spines in visual cortex in vivo: Changes during the critical period and effects of visual deprivation. *Proc. Natl. Acad. Sci. U.S.A.* **100**, 16024–16029 (2003).

53. C. L. Peebles, J. Yoo, M. T. Thwin, J. J. Palop, J. L. Noebels, S. Finkbeiner, Arc regulates spine morphology and maintains network stability in vivo. *Proc. Natl. Acad. Sci. U.S.A.* **107**, 18173–18178 (2010).

54. E. Messaoudi, T. Kanhema, J. Soulé, A. Tiron, G. Dagyte, B. da Silva, C. R. Bramham, Sustained Arc/Arg3.1 synthesis controls long-term potentiation consolidation through regulation of local actin polymerization in the dentate gyrus in vivo. *J. Neurosci.* **27**, 10445–10455 (2007).

55. T. Tsubota, R. Okubo-Suzuki, Y. Ohashi, K. Tamura, K. Ogata, M. Yaguchi, M. Matsuyama, K. Inokuchi, Y. Miyashita, Cofilin1 controls transcolumnar plasticity in dendritic spines in adult barrel cortex. *PLOS Biol.* **13**, e1002070 (2015).

56. G. Silasi, D. Xiao, M. P. Vanni, A. C. Chen, T. H. Murphy, Intact skull chronic windows for mesoscopic wide-field imaging in awake mice. *J. Neurosci. Methods* **267**, 141–149 (2016).

57. B. R. White, A. Q. Bauer, A. Z. Snyder, B. L. Schlaggar, J.-M. Lee, J. P. Culver, Imaging of functional connectivity in the mouse brain. *PLOS ONE* **6**, e16322 (2011).

58. S. R. Arridge, M. Cope, D. T. Delpy, The theoretical basis for the determination of optical pathlengths in tissue: Temporal and frequency analysis. *Phys. Med. Biol.* **37**, 1531–1560 (1992).

59. J. R. Bumstead, A. Q. Bauer, P. W. Wright, J. P. Culver, Cerebral functional connectivity and Mayer waves in mice: Phenomena and separability. *J. Cereb. Blood Flow Metab.* **37**, 471–484 (2017).

60. A. Q. Bauer, A. W. Kraft, P. W. Wright, A. Z. Snyder, J.-M. Lee, J. P. Culver, Optical imaging of disrupted functional connectivity following ischemic stroke in mice. *Neuroimage* **99**, 388–401 (2014).

Citation: A. W. Kraft, A. Q. Bauer, J. P. Culver, J.-M. Lee, Sensory deprivation after focal ischemia in mice accelerates brain remapping and improves functional recovery through Arc-dependent synaptic plasticity. *Sci. Transl. Med.* **10**, eaag1328 (2018).

Kraft *et al.*, *Sci. Transl. Med.* **10**, eaag1328 (2018)   31 January 2018

10 of 10

Science Translational Medicine

Sensory deprivation after focal ischemia in mice accelerates brain remapping and improves functional recovery through Arc-dependent synaptic plasticity

Andrew W. Kraft, Adam Q. Bauer, Joseph P. Culver and Jin-Moo Lee

Sensing a better approach for treating stroke

Brain injury due to ischemic stroke is a major cause of permanent behavioral disabilities. The effects of rehabilitation therapies are difficult to predict, and recovery is often incomplete. After cerebral ischemic stroke, spontaneous neuronal reorganization called remapping occurs in the area surrounding the injury and has been associated with functional recovery. Here, Kraft *et al.* show that sensory deprivation in mice (through whisker trimming) after focal cerebral ischemia improved sensorimotor recovery through accelerated remapping to the somatosensory cortex representing the whiskers. They demonstrate that a key player in this process is the protein Arc, which is known to be associated with synaptic plasticity. The results suggest that sensory deprivation might facilitate sensorimotor recovery after cerebral ischemia by promoting remapping of the injured region.

ARTICLE TOOLS	http://stm.sciencemag.org/content/10/426/eaag1328
SUPPLEMENTARY MATERIALS	http://stm.sciencemag.org/content/suppl/2018/01/29/10.426.eaag1328.DC1
RELATED CONTENT	http://stm.sciencemag.org/content/scitransmed/9/400/eaai9084.full http://stm.sciencemag.org/content/scitransmed/8/330/330re1.full http://stm.sciencemag.org/content/scitransmed/7/299/299ra121.full http://stm.sciencemag.org/content/scitransmed/9/399/eaah3621.full http://stm.sciencemag.org/content/scitransmed/10/432/eaao1313.full http://stm.sciencemag.org/content/scitransmed/10/441/eaao6459.full http://science.sciencemag.org/content/sci/360/6395/1349.full http://science.sciencemag.org/content/sci/361/6399/231.full http://stm.sciencemag.org/content/scitransmed/12/552/eaaz7287.full
REFERENCES	This article cites 60 articles, 18 of which you can access for free http://stm.sciencemag.org/content/10/426/eaag1328#BIBL
PERMISSIONS	http://www.sciencemag.org/help/reprints-and-permissions

Use of this article is subject to the Terms of Service